AGU100 ADVANCING EARTH AND SPACE SCIENCE

Geophysical Research Letters

RESEARCH LETTER
10.1029/2018GL079687

Key Points:
- Ra-age technique is suitable for hydrodynamic assessments in river-reservoir systems where model assumptions are met
- Sediment and nutrient retentions may be quantified using Ra water *ages*
- Nutrients are added and/or removed at different rates within three identified zones of the reservoir

Supporting Information:
- Supporting Information S1
- Data Set S1

Correspondence to:
Z. Yu,
zhigangyu@ouc.edu.cn

Citation:
Xu, B., Yang, D., Yao, P., Burnett, W. C., Ran, X., Charette, M., et al. (2018). A new perspective for assessing water transport and associated retention effects in a large reservoir. *Geophysical Research Letters*, *45*, 9642–9650. https://doi.org/10.1029/2018GL079687

Received 21 JUL 2018
Accepted 30 AUG 2018
Accepted article online 4 SEP 2018
Published online 23 SEP 2018

A New Perspective for Assessing Water Transport and Associated Retention Effects in a Large Reservoir

Bochao Xu[1,2], Disong Yang[1,3], Peng Yao[1,2], William C. Burnett[4], Xiangbin Ran[5], Matthew Charette[6], Xinying Huang[1,3], Sumei Liu[1,2], and Zhigang Yu[1,2]

[1]Key Laboratory of Marine Chemistry Theory and Technology, Ministry of Education, Ocean University of China, Qingdao, China, [2]Laboratory for Marine Ecology and Environmental Science, Qingdao National Laboratory for Marine Science and Technology, Qingdao, China, [3]College of Chemistry and Chemical Engineering, Ocean University of China, Qingdao, China, [4]Department of Earth, Ocean, and Atmospheric Science, Florida State University, Tallahassee, FL, USA, [5]Research Center for Marine Ecology, First Institute of Oceanography, State Oceanic Administration, Qingdao, China, [6]Department of Marine Chemistry and Geochemistry, Woods Hole Oceanographic Institution, Woods Hole, MA, USA

Abstract Radioactive tracer techniques may be useful for assessing water transport and the overall effects of concurrent biogeochemical processes in river-reservoir systems. In this study, we show that radium isotopes can assess the hydrodynamics and sediment/nutrient retention in the Xiaolangdi Reservoir, the largest impoundment along the Yellow River, China. Activity ratios of $^{224}Ra/^{226}Ra$ and $^{223}Ra/^{226}Ra$ were used for water mass *age* calculations in the riverine, transition, and lentic reaches of the reservoir. Water ages were combined with the length scale of three river-reservoir zones to determine water transport rates of 3.6 ± 1.2, 1.3 ± 0.3, and 0.16 ± 0.14 km/day, respectively. Radium ages were also used to quantify the net retention of sediment and nutrients in different parts of the river-reservoir system. Suspended sediment was removed at a rate of 1.4 ± 0.6 g/m^3/day, mainly in the riverine zone. Nutrient dynamics were more complicated, with addition or removal at different rates within the three zones.

Plain Language Summary This paper should be of interest to fluvial aquatic scientists and resource managers. Typically, numerical models have been used to estimate reservoir hydrodynamics, and associated biogeochemical processes are investigated separately. Here for the first time, we explore the validity of using radium isotope tracers to assess water age distributions in the Xiaolangdi Reservoir, the largest impoundment along the Yellow River (China). Radium ages were then used to quantitatively evaluate the net retentions of suspended sediments and nutrients within the reservoir. The technique is easy to conduct at relatively low cost and allows one to assess the overall effect of synchronized biogeochemical processes.

1. Introduction

In large river systems, the construction of dams and reservoirs for the purpose of water and sediment regulation significantly alters natural riverine hydraulic conditions. Depending on the water regulation scheme, river damming often results in the transformation of upstream water bodies from a natural riverine ecosystem to a lentic, or lake-like, reservoir (Friedl & Wüest, 2002). When river water discharges into a reservoir, water transport rates decrease, leading to settling of suspended particles and an increase in water transparency. Under such weakening hydrodynamic conditions, nutrient transformation processes are more effective and thoroughly developed within the reservoir. Consequently, such reservoirs tend to act as a *sediment filter* and/or a *biogeochemical reactor* for the river.

To improve our understanding of hydrologic-ecologic links in river systems, hydrologic conditions should be characterized in parallel with biogeochemical and ecological properties (Jones et al., 2017; Straškraba, 1999). To date, biogeochemical investigations and hydrodynamic simulations have usually been performed separately. Only rarely have there been endeavors to match these two studies simultaneously, mainly because of different research strategies. It has been shown, however, that nutrient removal in estuaries can be quantitatively estimated based on the relationship between nutrient concentrations and derived water transport rates (Peterson et al., 2009; Xu et al., 2016).

Water age is a commonly used time scale for first-order descriptions of water transport in reservoirs (Delhez et al., 2014; Monsen et al., 2002). It is suitable for quantifying, with high spatial resolution, the time history of a water mass (de Brauwere et al., 2011; Qi et al., 2016). In the case of rivers, lakes, and reservoirs, age is commonly computed with numerical (e.g., particle tracking) models (e.g., Bolin & Rodhe, 1973; Qi et al., 2016; Shen & Haas, 2004), occasionally assisted by use of passive dyes (Li et al., 2015) or stable isotopes (Birkel & Soulsby, 2016). In marine systems, besides modeling approaches, radioactive tracer techniques have been widely applied for age assessment (Delhez et al., 2003; England & Maier-Reimer, 2001). For example, during the past decade, the radium quartet and the *Apparent Radium Age Model* have been found to be useful tools for evaluating water ages in mostly marine settings including large river plumes extending into the coastal zone, estuaries, and over continental shelves (Charette et al., 2001; Dulaiova & Burnett, 2008; Moore, 2000; Xu et al., 2016). It is a convenient and low-cost technique for depicting water age distribution and plume trajectories (Xu et al., 2013).

Here we explore the validity of using radium isotope tracers to assess hydrodynamic processes through the perspective of water age distributions in a large river reservoir. The Xiaolangdi Reservoir (XLDR), located in the lower reaches of the Yellow River, is used as a novel laboratory to test this approach. Radium isotopes have only rarely been applied in freshwater systems. While the XLDR is responsible for a large majority of the sediment yield of global proportions (Syvitski et al., 2005), the measured suspended particulate matter (SPM) concentrations are comparable to some other major rivers. The high radium concentrations at the entrance to the reservoir, likely from desorption from SPM, provide a prominent starting point, allowing one to observe decay of short-lived Ra isotopes (^{223}Ra, ^{224}Ra) with downstream transport. We examined radium isotope activities and distributions throughout the river-reservoir system. Water ages were calculated by using the Apparent Radium Age Model and used to quantitatively evaluate the net retention effects of suspended sediments and nutrients within the reservoir. The technique is easy to conduct at relatively low cost (1- to 2-day sampling and a few days of radium measurements) and allows one to assess the net effect of synchronized biogeochemical processes.

2. Materials and Methods

2.1. Study Area

The Yellow River is the second largest river in the world in terms of sediment delivery to the sea (Milliman & Meade, 1983; Wang et al., 2017). Since the 1950s, China has been making serious efforts to manage the river, and more than 3,000 reservoirs and dams have now been constructed in the river basin (Wang et al., 2007). The XLDR, the most downstream large reservoir, is located at the mouth of the final gorge within the middle reach of the river (Kong et al., 2017). With a total water storage capacity of 13 km^3 and a sediment storage capacity of 7.6 km^3, the XLDR controls 92% of the Yellow River basin area and almost all of its sediment (Wang et al., 2016). The construction of the XLDR was completed in 1999, and this has significantly altered the water and sediment discharge pattern of the Yellow River since it became fully operational in 2002 (Wang et al., 2017; Zhou et al., 2015). Storage levels in the reservoir fluctuate during the year (Figure S1 in the supporting information). Usually, the XLDR is operated under a high storage protocol before May in order to provide water for spring irrigation and ice jam control. During June and July (prior to the wet season), the water level in the reservoir is reduced to below the flood control level of 225 m in order to free up storage space. During the wet season from August to October, excess water is stored in the reservoir, and the reservoir storage is maintained at a high level until the following May (Kong et al., 2017).

2.2. Sampling and Analysis

We launched a 5-day sampling expedition to the XLDR from 11 to 15 June 2017. A sampling transect was set up along the river channel direction, starting from ~60 km upstream from the Xiaolangdi Dam (Figure 1). The river discharge recorded at the upstream Sanmenxia Hydraulic Station during this sampling period ranged from 494 to 552 m^3/s. Surface water samples were collected for SPM, radium isotopes (^{226}Ra, ^{223}Ra, and ^{224}Ra), and nutrient analysis. Nutrients reported here include dissolved inorganic nitrogen (DIN) as the sum of NO_3^-, NO_2^-, and NH_4^+; dissolved inorganic phosphorus as PO_4^{3-}; and dissolved reactive silicate (DRSi) as Si $(OH)_4$. Detail information about sampling and analysis are shown in supporting information Text S1 (Grasshoff et al., 1999; Kim et al., 2001; Luan et al., 2016; Moore & Arnold, 1996; Waska et al., 2008).

2.3. Apparent Radium Age Model

The *water radium age* is intended to represent the calculated time elapsed since the radium isotopes were added to the system and isolated from a source (Dulaiova & Burnett, 2008; Moore, 2000). These ages (t) are

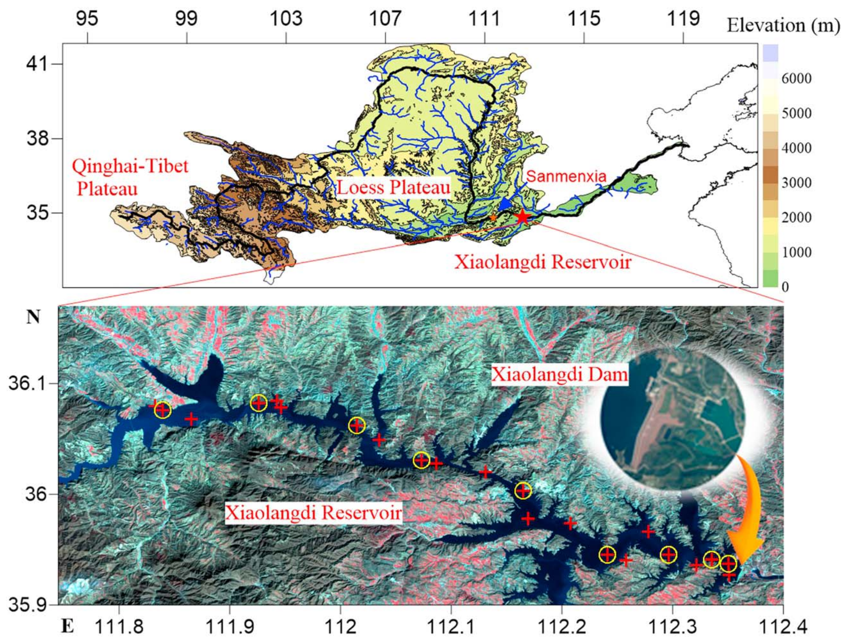

Figure 1. The study area of the Xiaolangdi Reservoir (top) and a more detailed sampling map for June 2017 (bottom). The red crosses are the Ra sampling sites, and the yellow-circled sites are where samples for suspended particulate matter and nutrients were also collected.

determined from the ratio of one of the shorter-lived radium isotopes to a longer-lived one. Use of a ratio corrects for any change by dilution or mixing, as both isotopes would be affected in the same manner. The radium ages are calculated from the following expression:

$$t = [\ln(AR_{obs}/AR_i)]/(\lambda_{long} - \lambda_{short}) \quad (1)$$

where AR_{obs} refers to the activity ratio of the Ra_{short}/Ra_{long} (e.g., $^{224}Ra/^{223}Ra$, $^{224}Ra/^{226}Ra$, and $^{223}Ra/^{228}Ra$) at a specific sampling location/time, while AR_i represents the initial Ra_{short}/Ra_{long} ratio at the suspected source. In our case, this initial ratio is taken from the sample with the highest activity ratio, which was collected near the entrance to the reservoir (i.e., presumably the one with minimum decay should be closest to a source). Thus, all ages are calculated relative to this location. The parameters λ_{long} and λ_{short} represent the decay constants of the long- and short-lived radium isotopes, respectively.

The radium age model approach has three basic assumptions: (1) the radium input is dominated by one source with a constant isotopic composition, (2) the losses of radium after leaving the source are only caused by mixing and radioactive decay, and (3) the downstream waters contain negligible amounts of excess ^{224}Ra and ^{223}Ra activities (Moore, 2000; Tomasky-Holmes et al., 2013). It is not necessary to require steady state conditions as long as the stated assumptions are satisfied. In our case, the data suggest that the assumptions are meant. More details regarding model assumption validity are shown in the supporting information Text S2 (Zhao & Wang, 2005).

2.4. Reservoir Retention Effects Model

Because of the dam/reservoir construction, water transport rates in the Yellow River have decreased. Concentrations of water transported materials, either dissolved (e.g., nutrients) or particulates (e.g., SPM), will be gradually changed (either by addition or removal) during downstream transport because of various physical and biogeochemical processes. To quantitatively estimate the apparent addition and/or removal rates of these substances within the river reservoir, we propose a simple model shown conceptually in Figure 2. The model is based on the relationship between material concentrations (C_t) versus water transport times (t) as follows:

$$C_t = C_0 - kt \quad (2)$$

where C_0 is the initial substance concentration at $t = 0$ and k is the retention coefficient, which is an apparent removal (or addition) rate for a certain parameter within the reservoir (units = concentration/day). Positive k

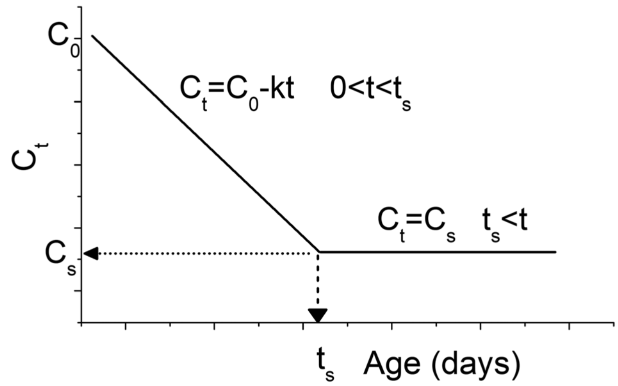

Figure 2. Conceptual sketch of the retention model. C_t is material concentrations when water transport time is t. C_0 and C_s are the initial and constant background levels of substance concentrations at $t = 0$ and $t > t_s$, respectively. k is the retention coefficient.

values represent a removal rate (negative k suggests addition), which is dependent on the combined effects of phytoplankton consumption, organic matter decomposition, suspended particles adsorption, or desorption and downstream mixing. The time, t, is the water transport time calculated by the radium model. The boundary condition is taken as when t is greater than 0 and less than t_s ($0 < t \leq t_s$). When $t > t_s$, water has flushed further downstream and the concentrations have reached steady state background levels. In this case, material concentrations may be expressed as $C_t = C_s$.

3. Results and Discussion

3.1. Radium Isotopes

All three measured radium isotopes (^{224}Ra, ^{223}Ra, and ^{226}Ra) show decreasing activity trends from upstream to the downstream XLDR, a consequence of mixing and radioactive decay processes (Figure 3). The zero distance shown in Figure 3 is the most upstream sampling location, about 60 km upstream of the Xiaolangdi Dam. The highest radium concentrations were found in the upstream river water, which passes through the Loess Plateau in the middle reaches of the river basin. The maximum time scale for a radioisotope tracer is approximately 5–6 half-lives of the isotope or a maximum of about 20 days for ^{224}Ra and 60 days for ^{223}Ra. The short-lived ^{224}Ra isotope was only detectable in the first 45 km. No measurable ^{224}Ra was detected within 15 km of the dam, indicating that the water ages within this section were all older than 20 days. The longer-lived ^{223}Ra also showed the most apparent reduction in the upper 45 km of the transect. However, the activities of ^{223}Ra in the last 15 km were still measurable, demonstrating that the water ages within this section were no greater than about 2 months. Long-lived ^{226}Ra (with a half-life of 1,600 years) would not decay under such short time scales, so the decrease of ^{226}Ra is mainly a consequence of mixing and dilution. It can thus serve as a *stable* tracer for the other radium isotopes.

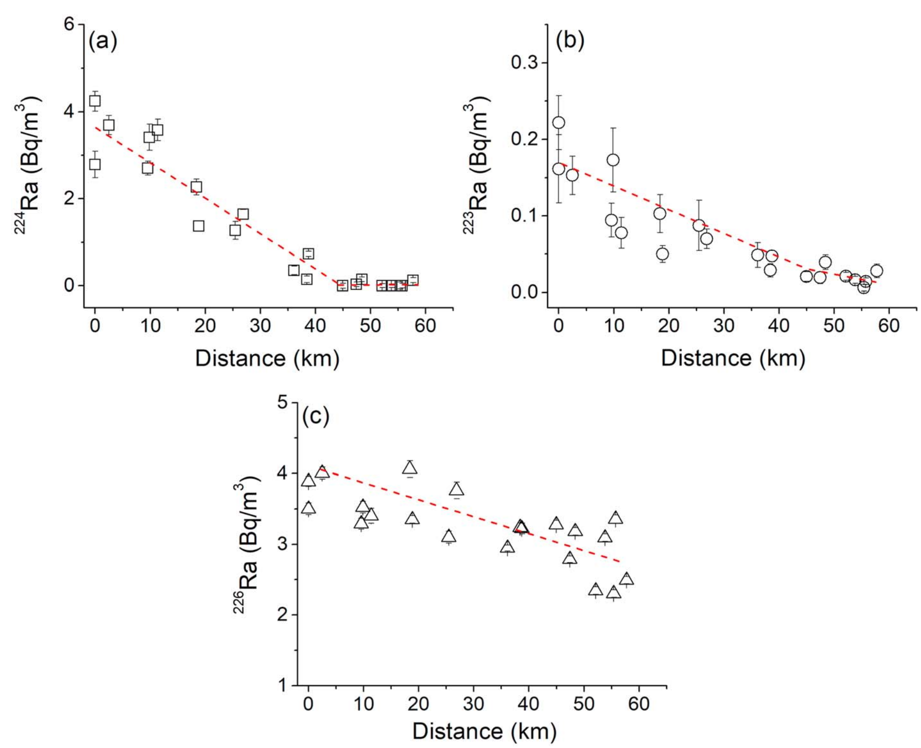

Figure 3. Activities of three radium isotopes, ^{224}Ra (a), ^{223}Ra (b), and ^{226}Ra (c) in the Xiaolangdi Reservoir river-reservoir system measured in June 2017. The uncertainties indicated are $\pm 1\sigma$ based on counting statistics.

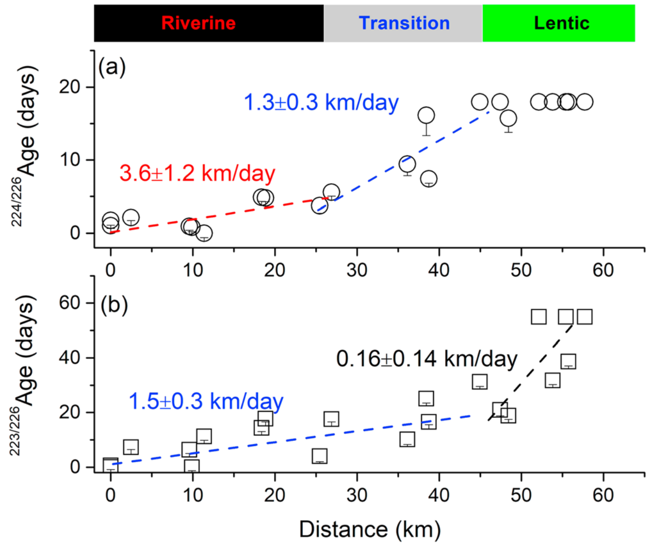

Figure 4. Apparent radium water ages in the Xiaolangdi Reservoir river-reservoir system during June 2017, based on $^{224}Ra/^{226}Ra$ ratios (a) and $^{223}Ra/^{226}Ra$ ratios (b). The upper (0–25 km), middle (25–45 km), and lower (45–60 km) sections of the Xiaolangdi Reservoir are now classified as riverine, transition, and lentic zones, respectively.

3.2. Radium Ages and Reservoir Zonation

The distributions of water ages traced by both the $^{224}Ra/^{226}Ra$ and $^{223}Ra/^{226}Ra$ activity ratios indicate a hydrodynamic zonation within the XLDR (Figure 4). In the upper 25 km, water ages based on $^{224}Ra/^{226}Ra$ ratios are all less than ~5 days, resulting in an overall water transport rate of 3.6 ± 1.2 km/day. In the middle section between 25 and 45 km, water ages gradually increased to the maximum tracing time scale (~20 days), suggesting a water transport rate of 1.3 ± 0.3 km/day. The water ages based on $^{223}Ra/^{226}Ra$ ratios in the first 45 km are somewhat more scattered and also gradually increase to about 20 days, resulting in an overall water transport rate of 1.5 ± 0.3 km/day. In the last section, from 45 km to the exit of the XLDR (Ra age ~60 days), the waters were very slow moving with calculated transport rates of only 0.16 ± 0.14 km/day. We also calculated the bulk water flushing time (75 days) by a classical approach and did a comparison to the radium age model result in supporting information Text S3. We consider the results based on these two methods that are comparable. The radium age model could offer more details about the ages distribution instead of a single bulk value, which is more useful to understand the hydraulic zonation of the reservoir.

Similar zonation characteristics have been previously reported in other river reservoirs, and riverine, transition, and lentic zones are considered a typical fluvial-to-lentic continuum (Hayes et al., 2017; Soares et al., 2008). The riverine zone is the region of the river-reservoir system located furthest from the dam, which is the first 25 km upstream in our case. It is characterized by an intense inflow of nutrients (Figure 5), other dissolved materials, and low primary production (Figure S2), as a result of rapid water flow and high turbidity. As sedimentation and light availability

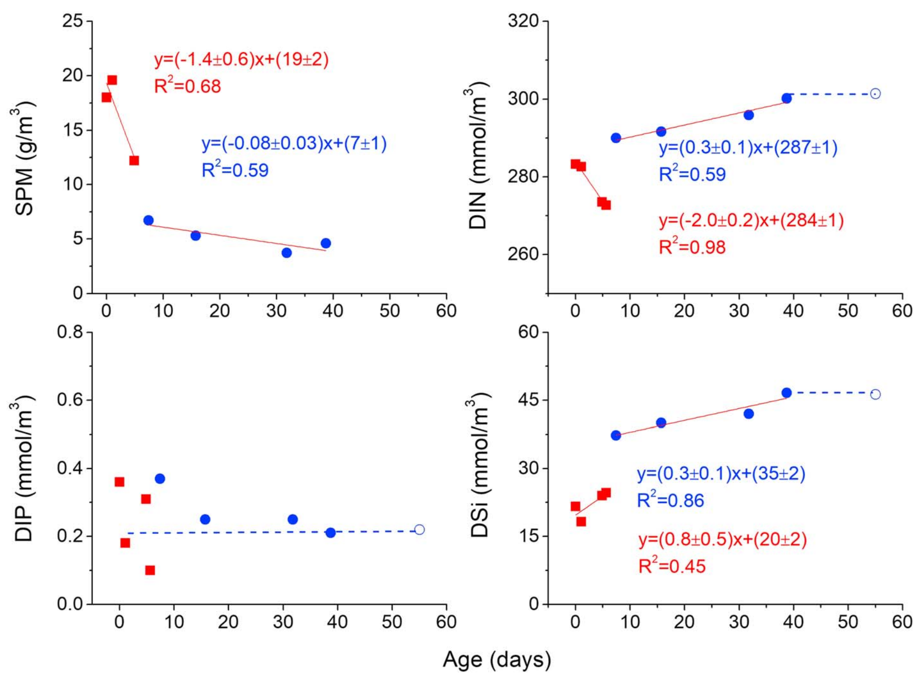

Figure 5. Concentrations of SPM and nutrients versus water ages in the XLDR river-reservoir system during June 2017. Red squares represent data from the riverine zone, and blue circles represent data from the transition and lentic zones. Open symbols and dashed lines indicate the zone with background concentrations when $t > t_s$. Water ages are based on $^{224}Ra/^{226}Ra$ ages for the first 45 km and $^{223}Ra/^{226}Ra$ ages from 45 km to the end of the reservoir. The ± values correspond to confidence level of 95%. SPM = suspended particulate matter; XLDR = Xiaolangdi Reservoir; DIN = dissolved inorganic nitrogen; DIP = dissolved inorganic phosphorus; DRSi = dissolved reactive silicate.

increase downstream, primary production increases within the transition zone. In XLDR, this zone is between 25 and 45 km with relatively low SPM concentrations (Figure 5), water flow rates, and increasing chlorophyll *a* (Figure S2). The final section is the lentic zone near the dam. Water ages in this section of the XLDR are older, at least 60 days relative to the most upstream sampling points (Figure 4). DIN and DRSi show enrichment downstream as SPM decreases (Figure 5), leading to an increase in productivity as shown by the increased chlorophyll *a* and dissolved oxygen (Figure S2).

3.3. Retention Effects

To quantitatively assess the retention effect within different sections of the reservoir, we applied the retention model by plotting nutrient and SPM concentrations versus apparent water ages (Figure 5). During the period of our investigation, the XLDR behaved as a net filter of suspended particles. Within the first 5 days, suspended particles were removed at a rate of 1.4 ± 0.6 g/m^3/day, equal to about 75% removal of the total suspended sediment load within this riverine section. This is consistent with Wang et al. (2010), who reported that after the Yellow River passed the XLDR, both the annual sediment load (40 Mt/year) and median grain size (6 μm) decreased significantly compared to the upstream values (400 Mt/year and 25 μm). Biogeochemical processes for nutrients were more variable within the different sections of the reservoir. In the fluvial section, DIN was removed at rates of 2.0 ± 0.2 mmol/m^3/day. DRSi, however, was added with a rate about 0.8 ± 0.5 mmol/m^3/day. Apparently, different nutrients are controlled by different biogeochemical processes. Since the observed nutrient behavior was a net result of several contributions and removal processes taking place under different spatial and temporal scales, we are not able to interpret the nutrient data based solely on a single process. The *net retention* dynamics assessed by our radium age approach is actually mixed nutrient signal occurring within the residence time of water in different sections of the reservoir.

In the transition section with water ages between 5 and 40 days, suspended particles were removed at a much slower rate of about 0.08 ± 0.03 g/m^3/day. Both DIN and DRSi were added to the water in this zone at a very similar rate of about 0.3 ± 0.1 mmol/m^3/day, implying that this addition may be resulted from decomposition and transformation of organic matter. In the lentic zone close to the Xiaolangdi Dam, we observed no further change in the DIN, dissolved inorganic phosphorus, and DRSi concentrations. Possible reasons for the observed nutrient behavior are discussed in the supporting information Text S4 (Hecky & Kilham, 1988; Justic et al., 1995; Li, 2017; Ran et al., 2015, 2018; They et al., 2017; Wang et al., 2010). We also calculated nutrient retention fluxes using a traditional approach and found that the estimate is comparable to the radium age approach result (supporting information Text S5). We think that the Ra age approach is actually preferable, because it does not rely on hydraulic gaging results, and can evaluate nutrient retention with high spatial resolution in the river-reservoir system.

3.4. Model Uncertainty and Application

Uncertainties associated with Ra-based water mass ages stem from the analytical uncertainty of radium isotopic measurements as well as possible departures from model assumptions. Reported analytical uncertainties are associated with measurement replications, counting statistics, and uncertainty propagation. In practice, relative analytical uncertainties of field samples analyzed by RaDeCC are usually on the order of 5% to 40% (Garcia-Solsona et al., 2008; Peterson et al., 2008). In our case, the analytical uncertainties for ^{226}Ra, ^{224}Ra, and ^{223}Ra ranged from 2% to 4%, 5% to 16%, and 16% to 40%, respectively. The higher ranges of analytical uncertainty (30% to 40%) are usually associated with very low activity cases, for example, $<$0.2 Bq/m^3 for ^{224}Ra and ^{223}Ra.

Ideally, the radium age model is suitable for one-entrance-one-exit reservoirs where the entrance represents a single source of radium and stratification is intense. Once the water entered the reservoir, dissolved radium would simply decrease by radioactive decay and mixing (Figure S3a). If there are large tributaries within the reservoirs, there could be additional radium sources that would invalidate the calculated ages. However, the entire reservoir system could be separated into a few sections. The model might still be valid within each section (Figure S3b). However, if there are too many tributaries and there is no clear radium decay observed in between, the model application would be limited. This is also true for rivers with multiple reservoirs in row (Figure S3c). Water discharged out of the uppermost reservoir should have low radium (short lived) because of decay during transportation inside the reservoir. Before entering the next reservoir, dissolved radium in the river would be recharged because of pore water release and sediment desorption. So the Ra age model could even be applied to a series of reservoirs separately, which would benefit the understanding of hydrodynamics in major rivers with intense human regulation. Of course, in whatever cases, the model assumptions should be tested.

In shallow reservoirs, especially when there are strong episodic disturbances (e.g., storms or hurricanes), enhanced physical mixing could introduce additional radium from bottom sediments. In reservoirs where radium inputs may occur throughout the system, the age model would provide only a lower limit age estimate. To account for this shortcoming, Moore et al. (2006) previously formulated another more explicit *Continuous Input* model, which was based on the activity ratios of the isotopes entering the system (Tomasky-Holmes et al., 2013).

The biogeochemical behavior of aquatic ecosystems depends, to a large extent, on the water transport and mixing dynamics that occur within them (Rueda et al., 2006). Lower discharge rates would allow coarser particles to settle more effectively while water flushed downstream. Nutrient concentrations and speciation could also be changed during downstream transport (Garnier et al., 1999; Kõiv et al., 2011; Ran et al., 2016). However, nutrients and SPM retention or release are usually calculated as an integrated parameter based on the difference between the inflow and outflow to the reservoir (Maavara, 2017). By using our proposed retention model, the results of nutrient and SPM removal and/or addition within the different hydraulic zones of the reservoir may be assessed. Water-transported materials may show quite different behaviors within each zone of the river-reservoir system. Both reaction rates and directions could vary under different hydrodynamic conditions. By using the radium age approach, one can not only quantify the overall retention effects but also consider the various zones and related hydrodynamics. Even for nonconservative species like nutrients, understanding their apparent retention or addition dynamics is very useful, especially for fluvial aquatic scientists and resource managers.

4. Conclusions

Water exchange and ecological responses in human-influenced major river reservoirs are of keen interest to the scientific community. However, biogeochemical investigations and hydrodynamic simulations have usually been performed as separate studies. In this study, we found that radium isotopes are suitable tracers to assess both water transport and the overall effects of concurrent sediment/nutrient retention in the XLDR, the largest river-reservoir system along the Yellow River. Water transport rates based on activity ratios of ^{224}Ra/^{226}Ra and ^{223}Ra/^{226}Ra were 3.6 ± 1.2 km/day, 1.3 ± 0.3 km/day, and 0.16 ± 0.14 km/day in the riverine, transition, and lentic reaches of the Xiaolangdi Reservoir, respectively. Radium ages were used to quantitatively evaluate the retention dynamics of sediment and nutrients in different parts of the system. SPM was removed at a rate of 1.4 ± 0.6 g/m^3/day, mainly in the riverine zone. Nutrient dynamics were more complicated, with addition and/or removal at different rates in the three zones of the reservoir. In the future, the Ra-age approach should be considered by aquatic scientists and resource managers for assessment of the hydrodynamics and associated biogeochemical processes in large river reservoirs.

Acknowledgments
We are grateful to Wu Xiao for his assistance during sample collection. The authors from Ocean University of China were funded by the National Key Research and Development Program of China (grant 2016YFA0600902), the National Science Foundation of China (NSFC grants 41576075, 41876075, and 41521064), the Aoshan Science and Technology Innovation Foundation (2016ASKJ02), and the Grand Master Program (MS2014ZGHY028). Radium and nutrient data can be found in the additional supporting information data sets S1 and S2.

References

Birkel, C., & Soulsby, C. (2016). Linking tracers, water age and conceptual models to identify dominant runoff processes in a sparsely monitored humid tropical catchment. *Hydrological Processes*, *30*(24), 4477–4493. https://doi.org/10.1002/hyp.10941

Bolin, B., & Rodhe, H. (1973). A note on the concepts of age distribution and transit time in natural reservoirs. *Tellus*, *25*, 58–62.

de Brauwere, A., de Brye, B., Blaise, S., & Deleersnijder, E. (2011). Residence time, exposure time and connectivity in the Scheldt Estuary. *Journal of Marine Systems*, *84*(3-4), 85–95. https://doi.org/10.1016/j.jmarsys.2010.10.001

Charette, M. A., Buesseler, K. O., & Andrews, J. E. (2001). Utility of radium isotopes for evaluating the input and transport of groundwater-derived nitrogen to a Cape Cod estuary. *Limnology and Oceanography*, *46*(2), 465–470. https://doi.org/10.4319/lo.2001.46.2.0465

Delhez, É. J. M., Brye, B. D., Brauwere, A. D., & Deleersnijder, É. (2014). Residence time vs influence time. *Journal of Marine Systems*, *132*, 185–195. https://doi.org/10.1016/j.jmarsys.2013.12.005

Delhez, É. J. M., Deleersnijder, E., Mouchet, A., & Beckers, J. M. (2003). A note on the age of radioactive tracers. *Journal of Marine Systems*, *38*(3-4), 277–286. https://doi.org/10.1016/S0924-7963(02)00245-2

Dulaiova, H., & Burnett, W. C. (2008). Evaluation of the flushing rates of Apalachicola Bay, Florida via natural geochemical tracers. *Marine Chemistry*, *109*(3-4), 395–408. https://doi.org/10.1016/j.marchem.2007.09.001

England, M. H., & Maier-Reimer, E. (2001). Using chemical tracers to assess ocean models. *Reviews of Geophysics*, *39*(1), 29–70. https://doi.org/10.1029/1998RG000043

Friedl, G., & Wüest, A. (2002). Disrupting biogeochemical cycles—Consequences of damming. *Aquatic Sciences*, *64*(1), 55–65. https://doi.org/10.1007/s00027-002-8054-0

Garcia-Solsona, E., Garcia-Orellana, J., Masqué, P., & Dulaiova, H. (2008). Uncertainties associated with ^{223}Ra and ^{224}Ra measurements in water via a Delayed Coincidence Counter (RaDeCC). *Marine Chemistry*, *109*(3-4), 198–219. https://doi.org/10.1016/j.marchem.2007.11.006

Garnier, J., Leporcq, B., Sanchez, N., & Philippon, X. (1999). Biogeochemical mass-balances (C, N, P, Si) in three large reservoirs of the Seine basin (France). *Biogeochemistry*, *47*, 119–146.
Grasshoff, K., Kremling, K., & Ehrhardt, M. (1999). *Methods of seawater analysis* (3rd ed., p. 600). Chichester, UK: John Wiley.
Hayes, N. M., Deemer, B. R., Corman, J. R., Razavi, N. R., & Strock, K. E. (2017). Key differences between lakes and reservoirs modify climate signals: A case for a new conceptual model. *Limnology and Oceanography Letters*, *2*(2), 47–62. https://doi.org/10.1002/lol2.10036
Hecky, R. E., & Kilham, P. (1988). Nutrient limitation of phytoplankton in freshwater and marine environments: A review of recent evidence on the effects of enrichment. *Limnology and Oceanography*, *33*, 796–822.
Jones, A. E., Hodges, B. R., McClelland, J. W., Hardison, A. K., & Moffett, K. B. (2017). Residence time-based classification of surface water systems. *Water Resources Research*, *53*, 5567–5584. https://doi.org/10.1002/2016WR019928
Justic, D., Rabalais, N., Turner, R., & Dortch, Q. (1995). Changes in nutrient structure of river-dominated coastal waters: Stoichiometric nutrient balance and its consequences. *Estuarine, Coastal and Shelf Science*, *40*(3), 339–356. https://doi.org/10.1016/S0272-7714(05)80014-9
Kim, G., Burnett, W. C., Dulaiova, H., Swarzenski, P. W., & Moore, W. S. (2001). Measurement of ^{224}Ra and ^{226}Ra activities in natural waters using a radon-in-air monitor. *Environmental Science & Technology*, *35*(23), 4680–4683. https://doi.org/10.1021/es010804u
Kõiv, T., Nõges, T., & Laas, A. (2011). Phosphorus retention as a function of external loading, hydraulic turnover time, area and relative depth in 54 lakes and reservoirs. *Hydrobiologia*, *660*(1), 105–115. https://doi.org/10.1007/s10750-010-0411-8
Kong, D., Miao, C., Wu, J., Borthwick, A. G. L., Duan, Q., & Zhang, X. (2017). Environmental impact assessments of the Xiaolangdi Reservoir on the most hyperconcentrated laden river, Yellow River, China. *Environmental Science and Pollution Research*, *24*(5), 4337–4351. https://doi.org/10.1007/s11356-016-7975-4
Li, X. (2017). Impacts of human activities on nutrient transports in the Yellow River: A special role of water-sediment regulation, (Mater thesis of Ocean University of China, pp. 50). In Chinese with English Abstract.
Li, Y., Zhang, Q., & Yao, J. (2015). Investigation of residence and travel times in a large floodplain Lake with complex Lake–River interactions: Poyang Lake (China). *Water*, *7*(12), 1991–2012. https://doi.org/10.3390/w7051991
Luan, Q., Liu, S., Zhou, F., & Wang, J. (2016). Living coccolithophore assemblages in the Yellow and East China Seas in response to physical processes during fall 2013. *Marine Micropaleontology*, *123*, 29–40. https://doi.org/10.1016/j.marmicro.2015.12.004
Maavara, T. (2017). Perturbations to nutrient and carbon cycles by river damming, (PhD thesis of University of Waterloo, pp. 6).
Milliman, J. D., & Meade, R. H. (1983). World-wide delivery of river sediment to the oceans. *Journal of Geology*, *91*(1), 1–21. https://doi.org/10.1086/628741
Monsen, N. E., Cloern, J. E., Lucas, L. V., & Monismith, S. G. (2002). A comment on the use of flushing time, residence time and age as transport time scales. *Limnology and Oceanography*, *47*(5), 1545–1553. https://doi.org/10.4319/lo.2002.47.5.1545
Moore, W., Blanton, J., & Joye, S. (2006). Estimates of flushing times, submarine groundwater discharge, and nutrient fluxes to Okatee Estuary, South Carolina. *Journal of Geophysical Research*, *111*, C09006. https://doi.org/10.1029/2005JC003041
Moore, W. S. (2000). Ages of continental shelf waters determined from ^{223}Ra and ^{224}Ra. *Journal of Geophysical Research*, *105*(C9), 22,117–22,122. https://doi.org/10.1029/1999JC000289
Moore, W. S., & Arnold, R. (1996). Measurement of ^{223}Ra and ^{224}Ra in coastal waters using a delayed coincidence counter. *Journal of Geophysical Research*, *101*(C1), 1321–1329. https://doi.org/10.1029/95JC03139
Peterson, R., Burnett, W. C., Santos, I., Taniguchi, M., Ishitobi, T., & Chen, J. (2009). Bohai Sea coastal transport rates and their influence on coastline nutrient inputs. In M. Taniguchi, W. C. Burnett, Y. Fukushima, M. Haigh, & Y. Umezawa (Eds.), *From headwaters to the ocean: Hydrological changes and watershed management* (pp. 659–664). Kyoto, Japan: CRC Press-Taylor & Francis Group.
Peterson, R. N., Burnett, W. C., Taniguchi, M., Chen, J., Santos, I. R., & Misra, S. (2008). Determination of transport rates in the Yellow River-Bohai Sea mixing zone via natural geochemical tracers. *Continental Shelf Research*, *28*(19), 2700–2707. https://doi.org/10.1016/j.csr.2008.09.002
Qi, H., Lu, J., Chen, X., Sauvage, S., & Sanchez-Perez, J. (2016). Water age prediction and its potential impacts on water quality using a hydrodynamic model for Poyang Lake, China. *Environemental Science and Pollution Research*, *23*(13), 13,327–13,341. https://doi.org/10.1007/s11356-016-6516-5
Ran, X., Chen, H., Zang, J., Yu, Y., Liu, S., & Zheng, L. (2015). Variability in the composition and export of silica in the Huanghe River Basin. *Science China Earth Sciences*, *58*(11), 2078–2089. https://doi.org/10.1007/s11430-015-5064-z
Ran, X., Liu, J., Zang, J., Xu, B., Zhao, S., Wu, W., et al. (2018). Export and dissolution of biogenic silica in the Yellow River (Huanghe) and implications for the estuarine ecosystem. *Marine Chemistry*, *200*, 14–21. https://doi.org/10.1016/j.marchem.2018.02.001
Ran, X., Liu, S., Liu, J., Zang, J., Che, H., Ma, Y., & Wang, Y. (2016). Composition and variability in the export of biogenic silica in the Changjiang River and the effect of Three Gorges Reservoir. *Science of the Total Environment*, *571*, 1191–1199. https://doi.org/10.1016/j.scitotenv.2016.07.125
Rueda, F., Moreno-Ostos, E., & Armengol, J. (2006). The residence time of river water in reservoirs. *Ecological Modelling*, *191*(2), 260–274. https://doi.org/10.1016/j.ecolmodel.2005.04.030
Shen, J., & Haas, L. (2004). Calculating age and residence time in the tidal York River using three-dimensional model experiments. *Estuarine, Coastal and Shelf Science*, *61*(3), 449–461. https://doi.org/10.1016/j.ecss.2004.06.010
Soares, M. C. S., Marinho, M. M., Huszar, V. L. M., Branco, C. W. C., & Azevedo, S. M. F. O. (2008). The effects of water retention time and watershed features on the limnology of two tropical reservoirs in Brazil. *Lakes & Reservoirs: Research and Management*, *13*(4), 257–269. https://doi.org/10.1111/j.1440-1770.2008.00379.x
Straškraba, M. (1999). Retention time as a key variable of reservoir limnology. In T. G. Tundisi & M. Straskraba (Eds.), *Theoretical reservoir ecology and its applications* (pp. 385–410). Brazil: International Institute of Ecology, Brazilian Academy and Backhuys Publishers, São Carlos.
Syvitski, J., Vörösmarty, C., Kettner, A., & Green, P. (2005). Impact of humans on the flux of terrestrial sediment to the global coastal ocean. *Science*, *308*(5720), 376–380. https://doi.org/10.1126/science.1109454
They, N., Amado, A., & Cotner, J. (2017). Redfield ratios in inland waters: Higher biological control of C:N:P ratios in tropical semi-arid high water residence time lakes. *Frontiers in Microbiology*, *8*, 1505. https://doi.org/10.3389/fmicb.2017.01505
Tomasky-Holmes, G., Valiela, I., & Charette, M. A. (2013). Determination of water mass ages using radium isotopes as tracers: Implications for phytoplankton dynamics in estuaries. *Marine Chemistry*, *156*, 18–26. https://doi.org/10.1016/j.marchem.2013.02.002
Wang, H., Bi, N., Saito, Y., Wang, Y., Sun, X., Zhang, J., & Yang, Z. (2010). Recent changes in sediment delivery by the Huanghe (Yellow River) to the sea: Causes and environmental implications in its estuary. *Journal of Hydrology*, *391*(3-4), 302–313. https://doi.org/10.1016/j.jhydrol.2010.07.030
Wang, H., Wu, X., Bi, N., Li, S., Yuan, P., Wang, A., et al. (2017). Impacts of the dam-orientated water-sediment regulation scheme on the lower reaches and delta of the Yellow River (Huanghe): A review. *Global and Planetary Change*, *157*, 93–113. https://doi.org/10.1016/j.gloplacha.2017.08.005

Wang, H., Yang, Z., Saito, Y., Liu, J., Sun, X., & Wang, Y. (2007). Stepwise decreases of the Huanghe (Yellow River) sediment load (1950–2005): Impacts of climate change and human activities. *Global and Planetary Change*, *57*, 331–354.

Wang, Z., Xia, J., Li, T., Deng, S., & Zhang, J. (2016). An integrated model coupling open-channel flow, turbidity current and flow exchanges between main river and tributaries in Xiaolangdi Reservoir, China. *Journal of Hydrology*, *543*, 548–561. https://doi.org/10.1016/j.jhydrol.2016.10.023

Waska, H., Kim, S., Kim, G., Peterson, R., & Burnett, W. C. (2008). An efficient and simple method for measuring ^{226}Ra, together with ^{223}Ra and ^{224}Ra using the scintillation cell in a delayed coincidence counting system (RaDeCC). *Journal of Environmental Radioactivity*, *99*, 1859–1862.

Xu, B., Dimova, N., Zhao, L., Jiang, X., & Yu, Z. (2013). Determination of water ages and flushing rates using short-lived radium isotopes in large estuarine system, the Yangtze River Estuary, China. *Estuarine, Coastal and Shelf Science*, *121*, 61–68.

Xu, B., Yang, D., Burnett, W. C., Ran, X., Yu, Z., Gao, M., et al. (2016). Artificial water sediment regulation scheme influences morphology, hydrodynamics and nutrient behavior in the Yellow River estuary. *Journal of Hydrology*, *539*, 102–112. https://doi.org/10.1016/j.jhydrol.2016.05.024

Zhao, K., & Wang, X. (2005). The deposition feature in branch rivers in reservoir region of XLD project. *Research of Soil and Water Conservation*, *12*(5), 168–171. In Chinese with English abstract

Zhou, Y., Huang, H., Nanson, G. C., Huang, C., & Liu, G. (2015). Progradation of the Yellow (Huanghe) River delta in response to the implementations of a basin-scale water regulation program. *Geomorphology*, *243*, 65–74. https://doi.org/10.1016/j.geomorph.2015.04.023